UPTEC Q 23003
Examensarbete 30 hp
Juni 2023

UPPSALA UNIVERSITET

Impact of nanoparticle plasmons on photoluminescense and upconversion processes in ZnO

Axel Gudmundsson

Civilingenjörsprogrammet i teknisk fysik med materialvetenskap

UPPSALA UNIVERSITET

Impact of nanoparticle plasmons on photoluminescense and upconversion processes in ZnO

Axel Gudmundsson

Abstract

The increasing prevalence of glass windows in modern buildings has raised the demand for solar control windows that possess climate-appropriate properties. Glass windows made of abundant and low-cost materials which can both decrease the heating energy consumption as well as enhance the light climate indoors would sufficiently meet the goals of economical yet uplifting buildings. The main objective of this thesis was to examine whether a plasmonic hybrid interface, comprising three layers of thin films (gold nanoparticles of approximately 10 nm, ZrO_2 with a thickness range of 20-35 nm, and ZnO with a thickness of approximately 20 nm), could achieve the upconversion of infrared light to visible light through a multiphoton absorption process in the ZnO layer. If successful, this configuration, in conjunction with an established layer capable of downconverting ultraviolet light to visible light, would be applied to commercially available glass windows to enhance the solar utilization and improve indoor lighting conditions. ZnO was selected as the upconversion material due to its wide emission range in the visible spectrum, indicative of intermediate electron states between the valence and conduction bands suitable for excitation. The objective of the plasmonic material, the gold nanoparticles, was to increase the probability of the upconversion process by utilizing the enhanced electric field resulting from plasmons localized at the surface of the gold nanoparticles. ZrO_2 served as a separator layer between the plasmonic material and the ZnO, to effectively preventing charge transfer and ensuring that any upconversion or other photoluminescence processes were purely photonic. Various optical experimental techniques were employed in this study to assess any upconversion, plasmon enhancement, and map the intermediate electron states of the ZnO. The ZrO_2 layer successfully prevented charge transfer between the layers. However, the influence of the gold's surface plasmons and it's enhanced electric field on ZnO emission varied among the samples, likely due to the synthesis processes. Ultimately, the plasmonic hybrid interface investigated in this thesis did not exhibit detectable upconversion when illuminated with either 600 or 750 nm light. Further research is necessary to increase the density of intermediate electron states in ZnO, along with optimization of the thin film synthesis to enhance plasmon effects. These advancements would augment the probability of detectable upconversion.

Teknisk-naturvetenskapliga fakulteten

Uppsala universitet, Utgivningsort Uppsala

Handledare: Jacinto Sá

Ämnesgranskare: Carl Hägglund

Examinator: Lena Klintberg

Populärvetenskaplig sammanfattning

Impact of nanoparticle plasmons on photoluminescense and upconversion processes in ZnO

Axel Gudmundsson

Fler och fler arkitekter väljer att designa nya byggnader med en större andel glasfönster. Detta har resulterat i att funktionaliteten hos vanliga glasfönster till bostäder och andra lokaler har setts över. I strävan efter ett energieffektivare samhälle tillsammans med önskan att skapa en levande och arbetsvänlig miljö med generöst ljusflöde har forskning kring framtida glasfönster intensifierats.

Ett fönster som kan omvandla ljus osynligt för människans öga till synligt ljus var det huvudsakliga målet med detta projekt. Detta ska ske genom en så kallad uppkonverteringsprocess, där ett material skall absorbera 'osynligt', infrarött ljus, med lägre energi och konvertera detta till synligt ljus med högre energi. Slutligen innebär detta en högre mängd synligt ljus som genomstrålar och belyser inomhusmiljön.

- Hur går då en uppkonverteringsprocess till?

Om man föreställer sig att en elektron i sitt grundtillstånd befinner sig på marken och när den absorberar energi i form av ljus får den energi nog att hoppa upp på ett trappsteg upphöjt från marken, det vill säga en annan energinivå. Elektronen kan dock inte befinna sig i detta exciterade tillstånd särskilt länge och detta illustreras i Figur 1 nedan där trappstegen dras undan med tiden, vilket tvingar elektronen att hoppa ner och frigöra överskottsenergin genom att släppa ut ljus med samma energi igen. Denna process kallas fotoluminescens. Här har det alltså inte skett någon uppkonvertering, utan för att detta skall hända behöver den redan exciterade elektronen lyckas absorbera ytterligare en ljusvåg, även kallad foton, för att hoppa upp på nästa trappsteg. Denna andra absorption måste alltså ske innan trappsteget den står på försvinner under fötterna. Nästa trappsteg försvinner ännu snabbare och därmed sannolikheten att hoppa ännu ett trappsteg är minimal. Till slut tvingas elektronen från andra trappsteget att hoppa ner och därmed frigör den en foton med högre energi, denna process kallas uppkonvertering.

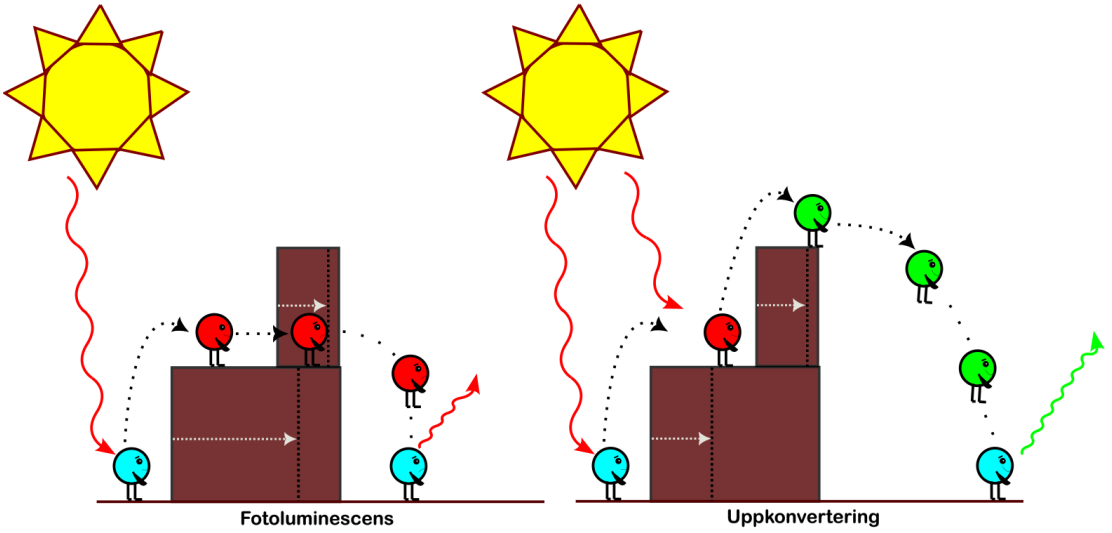

Figure 1 En illustration av processerna fotoluminescens och uppkonvertering.

Materialsammanställningen, bestående av tre tunna skikt, som undersöktes för uppkonvertering av lågenergi ljus i detta projekt bestod av följande: En tunnfilm av zinkoxid (ZnO), ett avskiljningslager bestående av zirkoniumdioxid (ZrO_2) och till slut ett lager av nanopartiklar av guld, som har en diameter kring en tiotusendel av tjockleken på ett vanligt A4 papper. När guldet utsätts för ljus med tillräckligt hög energi skapas något som kallas plasmoner, vilket är, kortfattat, en grupp elektroner som oscillerar synkroniserat. Dessa elektroner på ytan av guldnanopartiklarna genererar ett elektriskt fält i sin omgivning och detta elektriska fält i sin tur kan förstärka sannolikheten att en elektron absorberar en foton och därmed hoppar upp i energinivå. Man kan föreställa sig som att plasmonerna är ett gäng elektroner som agerar hejarklack, som hoppar och hejar på deltagarna (elektronerna i zinkoxiden). Syftet med zirkoniumdioxiden var att separera guld nanopartiklarna från Zinkoxiden för försäkra att ingen av elektronerna från hejarklacken kommer till zinkoxiden.

Med hjälp av en rad olika experimentella metoder som kan mäta ett materials diverse optiska egenskaper kunde flera intressanta slutsatser dras. Zirkoniumdioxiden fungerade som en bra isolator mellan hejarklack och deltagare, dock framstod hejarklackens påverkan på deltagarnas resultat olika mellan proverna. Någon uppkonvertering kunde tyvärr inte detekteras och därför krävs ytterliggare studier för att optimera skapandet av proverna så att plasmonernas hejande är mer konsekvent. Sedan skulle även förändring av zinkoxiden behöva göras så fler stora och tydliga trappsteg möjliggörs för elektronerna, vilket ökar sannolikheten för uppkonvertering.

List of Abbreviations

UV	Ultra-violet
IR	Infrared
Vis	Visible
SPR	Surface Plasmon Resonance
SPP	Surface Plasmon-polariton
LSP	Localized Surface Plasmon
LSPR	Localized Surface Plasmon Resonance
UPC	Upconversion
DC	Downconversion
SPDC	Spontaneous Parametric Photon Downconversion
TAS	Transient Absorption Spectroscopy
TRIR	Time Resolved Infrared Spectroscopy
TCSPC	Time-correlated Single Photon Counting
MCP	Micro Channel Plate
OPA	Optical Parametric Amplifier
SPCG	Super Continuum Generation
SE	Stimulated Emission
CW	Continuous Wave

Contents

1 Introduction

According to SBBA's Heating Market report which covers Sweden's energy consumption of 2020 a total of 43.1 TWh was used for district heating, where dwellings and non-residential buildings accounted for 58% [1]. The last couple of years the energy prices in Sweden has shown an unstable behaviour due to political and resource problems in Europe [2]. This motivates more energy efficient buildings which would decrease their environmental impact as well as their heating cost. There are several ways of reducing the energy consumption in buildings, common approaches are bettering insulation, ventilation and glass windows [3]. It has become a trend in Sweden and elsewhere to build facilities with a large amount of windows, not only because it is fashionable but also since glass windows allows an uplifting inside climate with a great deal of natural light. Consequently, there is a sizable demand for inexpensive, energy-efficient, and transparent for visible light glass windows.

Various research have displayed a wide range of different solar control windows today. Everything from thermochromic windows that decreases the transmission of infrared (IR) light at warmer temperatures to electrochromic windows that can change color with an applied bias as well as low emission coating windows that more effectively keeps the buildings temperature more stable due to IR light reflection. This project present research for a solar control window that can simultaneously convert high energy photons in the Ultra Violet (UV) region and low energy photons in the Infrared (IR) region to light in the visible region. By using plasmonic nanoparticles supposedly these conversions are enhanced and results in a larger throughput of visible light, improving the light climate inside buildings. A graphical illustration of how these solar control windows would work is shown in Figure 2 below.

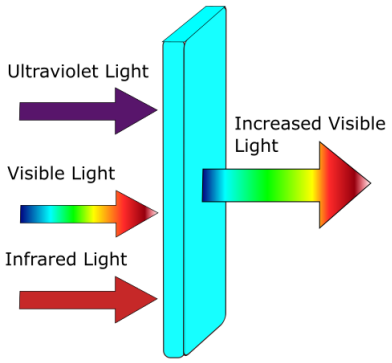

Figure 2 Elementary sketch illustrating how the conversion of UV and IR light increases the throughput of visible light.

Materials that possess the ability to down-convert ultraviolet light to visible light are currently available [4] [5]. Therefore, this project's prime focus was to present research on upconversion from infrared and the lower energy region of visible to visible light.

1.1 Aim

This projects aim was to conduct further research of the infrared to the visible light upconverting concepts with plasmonic hybrid interfaces. It is inspired by previous research that is currently under review pioneered in Prof. Jacinto Sá's group at Ångström Laboratory where infrared-to-visible photon upconversion was documented on $Plasmon/TiO_2$ solid films [6]. Instead of Titania which is known as a poor emitter, this project evaluated if the abundant and more famously emitting material ZnO is suitable for photon upconversion applications.

The following questions were under the magnifying glass in this project:

- What is the ZnO's emission and absorbance spectra and can a nearby plasmon-induced electric field enhance it's efficiency?
- What available intermediate so called 'trapped electron states' does ZnO possess between the valence band and the conduction band?
- If there is an enhancement of absorbance and emission due to a nearby plasmon-induced electric field, does the ZnO's intermediate electron states enable upconversion?

2 Background

2.1 Surface Plasmons

When free electrons at metals surfaces interact with an electric field of great enough energy a phenomena called surface plasmon resonance (SPR) occurs. A plasmon is a collective oscillation of excited electrons. These surface electron oscillations can be acknowledged as two different modes, one is the surface plasmon-polariton (SPP), which can move along the interface between the metal and a dielectric medium. The other is the one which will be discussed further in this paper and that is the localized surface plasmon (LSP) which is isolated around a nanoparticle/nanostructure [7].

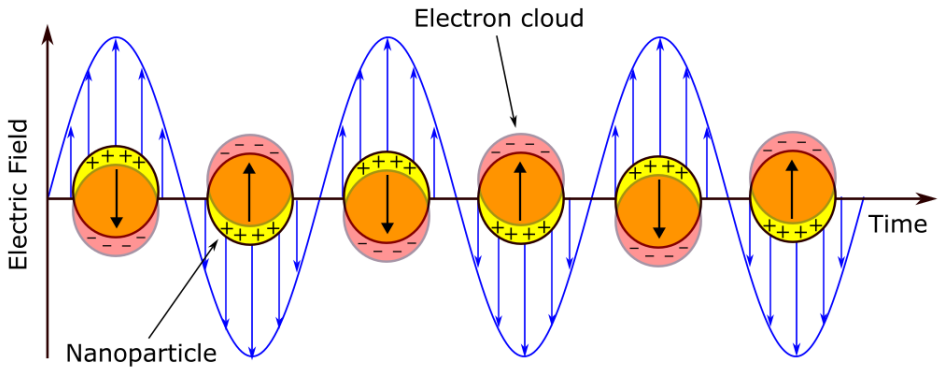

Figure 3 Graphical illustration of how an external electric field causes the electron clouds in the nanoparticle to oscillate, which is defined as the localized surface plasmon.

Localized surface plasmons contribute with two interesting effects, one is that the optical absorption is at it's maximum at the material's plasmon resonance frequency. By altering a material's shape, size and electron density it's possible to tune the plasmon resonance frequency. The other is that electric fields at the surface of the nanoparticle are enhanced significantly which can be utilized by nearby functional materials [7].

2.1.1 Hot carriers

As mentioned, the collective oscillation of a metal's conduction electrons i.e. the plasmon is generated by electromagnetic excitation. These electrons starts to scatter off of other electrons as well as the surface of the nanoparticle, this mechanism is called dephasing and takes place in a lifetime of femtoseconds. During this small timeframe

these scattered electrons excite other electrons and create charge carriers consisting of electrons and holes. Charge carriers created by plasmon dephasing are called 'hot carriers' and are susceptible for energy harvesting [9]. Because of their short lifetime the excess energy of these hot carriers have for long been complicated to harvest. If the excess energy is not harvested in the femtoseconds timeframe the carriers thermalize and heat the lattice by electron-phonon scattering. A way to take advantage of plasmons is to utilize the enhancement of their surrounding electric field. The plasmonic material works similar to an antenna, amplifying the 'signal' of the nearby material [9]. The 'signal' could be anything that is affected by an electric field, common and more discussed 'signals' such as absorption efficiency, excitation stability or density of electronic states will be further elaborated in this paper.

2.2 Photon Up-conversion

Through a multiphoton absorption process along with a material with appropriate available electronic states it is theoretically possible to emit light with a shorter wavelength than the incident incoming light. This is called photon up-conversion [10]. Looking back it has not been successful enough due to inefficient and complicated systems, only applicable with the help of powerful lasers. Now scientists and companies are trying to use plasmonic systems in order to increase the efficiency. An efficient photon up-conversion system would be applicable in multiple applications, two hot potential applications currently under the magnifying glass are windows and photovoltaics. Two common ways using plasmonic systems in up-conversion are the following: Plasmon induced charge transfer up-conversion and Plasmon-enhanced up-conversion [9] [10] [11].

2.2.1 Plasmon Induced charge transfer Up-conversion

This system usually consists of a metal (plasmonic material) and a semiconductor that acts as an emitter. The use of multiphoton absorption in plasmonic materials allows charge transfer of hot charge carriers to the semiconductor, where they recombine and emit photons. It is important that these systems consist of Schottky barriers (potential energy barriers for metal-semiconductor transitions) that are lower than the hot carrier energy level [10].

2.2.2 Plasmon-enhanced Up-conversion

In Plasmon-enhanced systems plasmonic nanoparticles are placed close to an up-conversion (UPC) material along with an intermediate layer to prevent charge transfer. What's special with an UPC material is that they possess several intermediate electron states, or so called trapped states, between the valence band and conduction band, where the electrons can be excited to and be trapped for a short period of time [13]. This enables a multiphoton absorption process, illustrated in Figure 4.

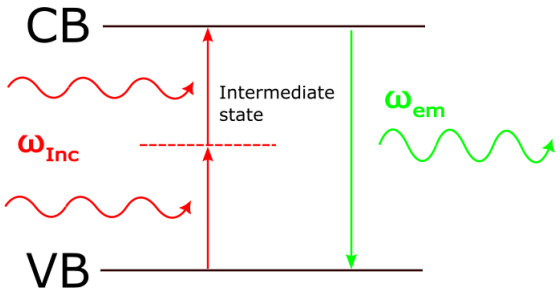

Figure 4 Schematics on how an intermediate electron state between the valence and the conduction band can enable multiphoton absorption, resulting with emission of a photon with greater energy.

In Plasmon-enhanced up-conversion there is no charge transfer, instead the plasmonic material works as an antenna. Sun light consist of all wavelengths in the visible region, including the plasmon resonance frequency of the plasmonic material. When light with the same wavelength as the materials plasmon resonance frequency reaches the nanoparticle it's electric field along the surface increases significantly [9]. This enhancement of the electric field increases the possibility of absorption and therefore exciting electrons of the nearby UPC material into trapped states. These excited electrons in the trapped states would then be available for another photon absorption, which can then relax and emit a photon with higher energy, visualised in Figure 5.

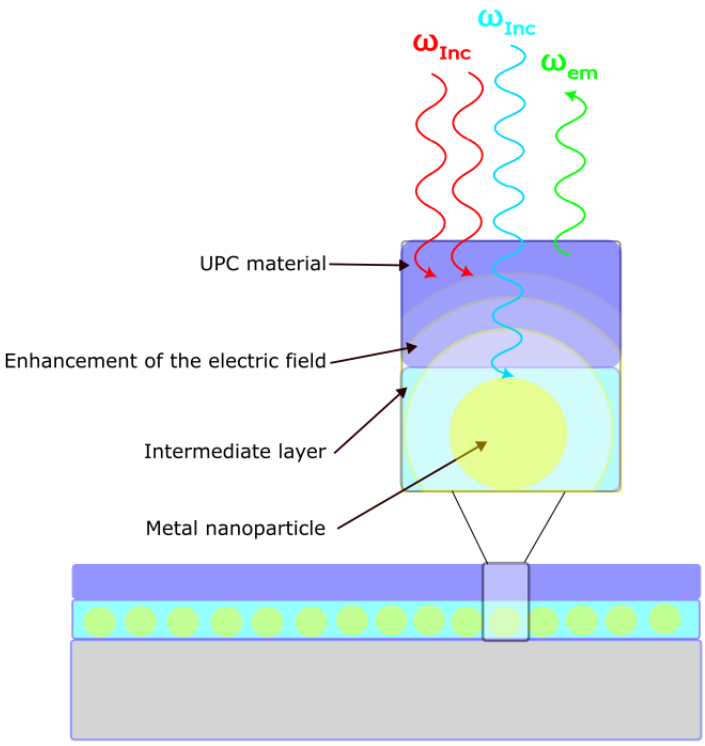

Figure 5 Practical illustration of a hybrid plasmon-enhanced up-conversion system.

In order to optimize a plasmon-enhanced up-conversion system, the thickness of the intermediate layer needs to be tuned. If there is too large of a distance between the plasmonic material and the UPC material the amplitude of the enhanced electric field would be too low. On the other hand, if the intermediate layer is too thin there is a risk of charge transfer. Figure 6 below illustrate how the intermediate layer's thickness should be optimized.

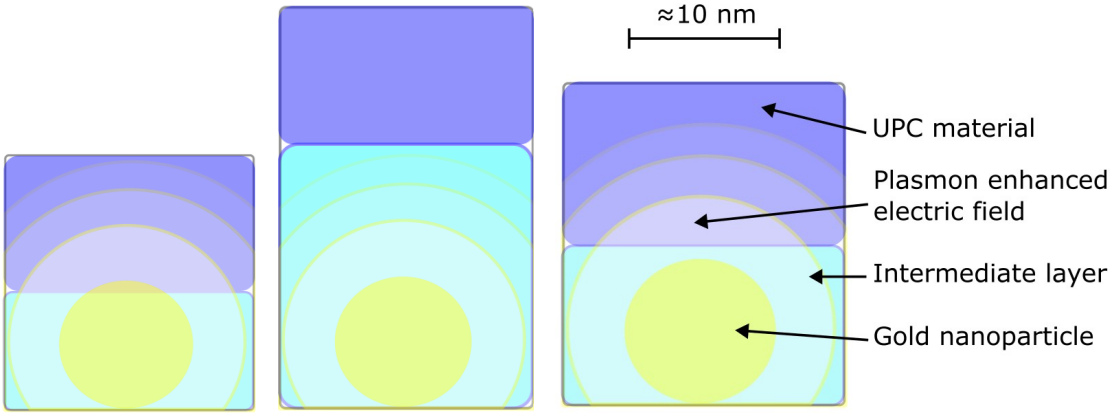

(a) Too thin. **(b)** Too thick. **(c)** Optimised.

Figure 6 a) Show how a too thin of an intermediate layer enables charge transfer. b) Demonstrate how the enhancement of the electric field won't reach the UPC material when the intermediate layer is too thick. c) Show how an optimized thickness of the intermediate layer disables charge transfer along with allowing the enhancement of the electric field reach the UPC material.

2.3 Spontaneous Parametric Photon Down-conversion

When a dielectric medium is exposed to an electric field of great enough magnitude nonlinear properties cannot be neglected anymore, causing a probability of frequency conversion. There are two types of frequency conversions, the first has already been mentioned, UPC, the other method is called Spontaneous parametric photon down-conversion (SPDC), which instead of absorbing a minimum of two lower energy photons and convert them into a higher energy single photon as in UPC, this phenomena does the reverse. That is, when the dielectric material is exposed to a high frequency electromagnetic field, it converts that single photon into a photon pair whose energy correlates with the energy of the incident photon according to the law of conservation of energy [14]. This is illustrated in Figure 7. What this means is that the angular momentum as well as the total energy is conserved from the single photon through to the photon pair. This knowledge has been used to answer fundamental questions in quantum mechanics as well as utilized in optical parametric amplifiers which will be explained in further depth in the experimental method part.

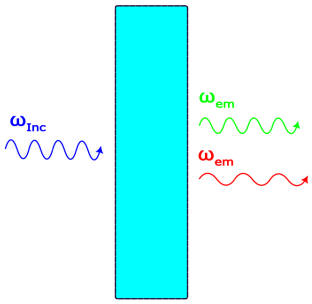

Figure 7 The DC material converts one high frequency photon into two photons with lower frequencies.

2.4 Previous Research and the Projects Vision

Plasmonic nanoparticles have previously been used for a large diversity of applications. Two common examples such as catalysts and photovoltaics are currently hot topics [8] [15]. Since the localised surface plasmon resonance frequency (LSPR) has been studied in a number of fields it has contributed to an overall greater understanding of it's theory as well as how it can be applicable. This project stems from wanting to discover if using LSP's can help their contribution of science to more efficient and smarter glass windows [6]. Many of the more developed glass windows of today use their technology in one way or another to reduce the amount of unwanted light that is transmitted, meaning at the moment there is no window that actually try to both decrease the unwanted light as well as increasing the transmitted light of the wanted wavelengths, such as visible light. The vision of this project was to create a set up, combining UPC and DC materials with an intermediate layer of gold nanoparticles as the plasmonic material. Figure 8 below illustrates the desired setup, which utilises the plasmon-enhanced surrounding electric field in both the down-conversion as well as the up-conversion of unwanted wavelengths to visible light.

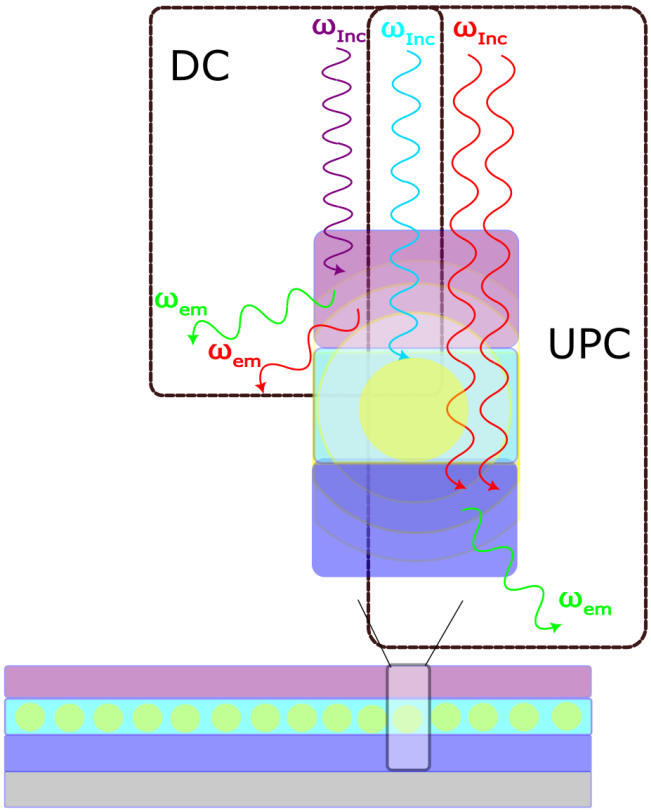

Figure 8 The desired structure that when optimised convert both UV and IR light to light in the visible region.

3 Instruments

There are various ways to measure a material's optical properties, common methods are absorption and fluorescence measurements. Both involves illuminating the sample with either a singular desired wavelength or a range of wavelengths. The absorption techniques measure the difference in intensity after illuminating the sample meanwhile the fluorescence techniques measure the emission from the material.

This section will go over the experimental instruments used in this project. The more basic instruments are discussed broadly while instruments that are more complicated are discussed in a detailed manner.

3.1 Absorption techniques

UV-Vis Spectrophotometer

One of the more older techniques to measure a sample's optical properties, specifically the absorbance is the 'Ultra violet to Visible light Spectrophotomer', commonly referred to as the 'UV-Vis Spectrophotometer'. The instrument can generally be understood with explanation of the most vital experimental parts. The parts are, A lamp (usually a deuterium or a tungsten lamp), a monochromator, a sample holder and a detector. Where the lamp generates wavelengths in a broad range which will reach the monochromator where only one wavelength is let through at a time and hit the sample. For each wavelength the detector interpret the change of reflectance, transmittance and scattering and infer this as absorption which then generate a wavelength dependent absorption spectra [16]. In this project this technique is used to qualitatively measure the concentration of gold nanoparticles distributed on the samples.

Time resolved infrared spectroscopy (TRIR)

When observing photoinduced reactions quite often transient absorption spectroscopy (TAS) are used. TAS involves a pump and probe methodology. The pump has a high intensity and it's objective is to excite as many electrons as possible when reaching the sample. This results in a negligibly low probability of further absorption, this state is called a transient state. Whereas the probe is used to measure the change of absorption at different times after the pulse of the pump, the probe can then gather information on how the materials occupied states behaves with time [18]. In this project Time Resolved Infrared Spectroscopy (TRIR) is used, which is a subcategory of TAS where the probe

has a wavelength in the infrared region. The purpose of using TRIR is to capture information about electron transfer. To validate that any enhancement due to the plasmonic material is purely photonic, the TRIR measurements are made to ensure that any charge transfer between the gold and the UPC material are prevented.

3.2 Fluorescence techniques

Fluorescence measurements are commonly classified into two different types: steady-state and time-resolved. Steady-state measurements illuminates the sample with a constant intensity for a longer period of time and an emission spectra is recorded. Meanwhile time-resolved measurements utilizes a pulse of light and then measure the fluorescence intensity decay [17].

3.2.1 Steady-state instruments

Spectrofluorometer

The spectrofluorometer consists of a similar setup as the UV-Vis spectrophotometer, a lamp, two monochromater, a sample holder and a detector. Meanwhile the spectrophotometer measures the absorption after the sample the spectrofluorometer measures the emission. The lamp generates a broad spectrum of wavelengths and the first monochromator transmits the desired excitation wavelength to the sample. As the sample is illuminated with the excitation wavelength the second monochromator slowly shifts, allowing emission from a range of wavelengths to be recorded with the detector and an emission spectra is generated [17]. In this project the fluorometer is used to evaluate the emission at different excitation wavelengths and to correlate the emission to the sample's electronic states.

3.2.2 Time Resolved instruments

Time-correlated Single Photon Counting (TCSPC)

One typical time-resolved fluorescence experiment is called Time-correlated Single Photon Counting (TCSPC), where the fluorescence detector measures the amount of photons emitted correlated to the time after the excitation pulse of light. This does not illustrate which wavelengths emitted, but an overview of the fluorescence decay intensity [17]. The previous mentioned Fluorometer and the TCSPC complement each other. The

Fluorometer's steady-state measurements gives you a quick overview of which wavelengths that are emitted as well as their average intensity meanwhile the time-resolved measurements can help you with information on the longevity of the different excited states.

Streak Cameras

In contrast to the TCSPC which can only measure the quantity of photons emitted, Streak cameras can also give information of the corresponding wavelength to the photon, meaning it will provide a 2D image with time on one axis and wavelength on the other. This enables a more detailed overview of the emissions from the sample. Another advantage the streak camera has over the TCSPC is that it is significantly faster, possessing an maximum temporal resolution of 0.2 ps which corresponds to the time it takes for light to travel 0.06 mm [19]. This ultra-fast detection allows you to gather information about short lived states which would not be detected in a TCSPC. Since the ability to use a wide range of excitation wavelengths is often preferable an Optic parametric amplifier (OPA) is commonly used.

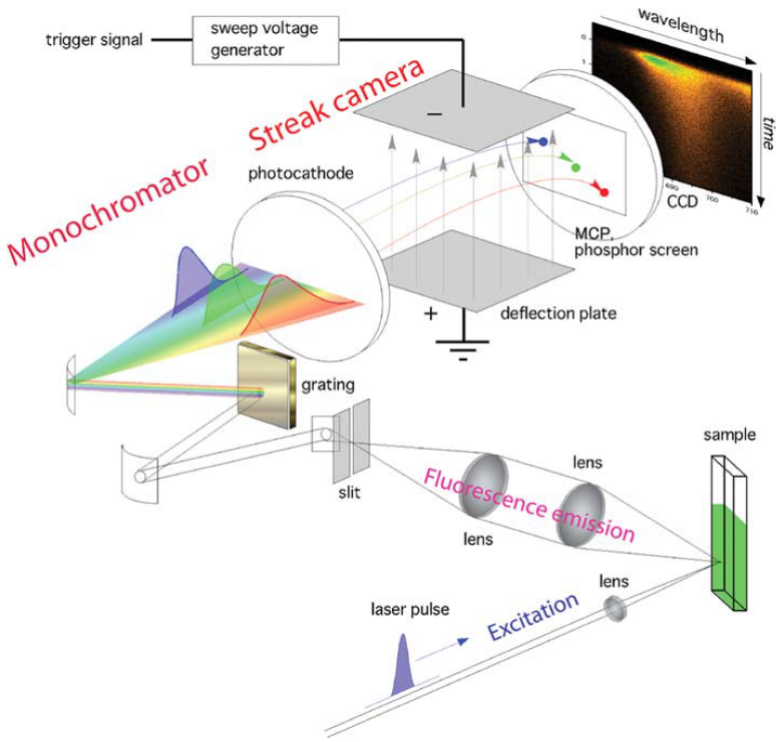

Figure 9 Schematics showing how the emitted light from the sample is measured in a streak camera[20].

Figure 9 shows the operating principle of the streak camera. How the emitted light leaves the sample and result with an image with both wavelength and time dependence. The emission from the sample is focused through a slit and then reflected to a grating in order to separate the light into their individual wavelength, essentially creating the wavelength axis. The light is then converted into electrons with a photocathode, where the amount of the electrons are proportional to the intensity. Furthermore the electrons are accelerated between two sweep electrodes which is time dependent and synchronized with the incident light, meaning at slightly different times the electrons will project in various angles, effectively giving them a time component which can be interpreted with a time axis. The electrons reaches the micro channel plate (MCP) where the signal is amplified by multiplying the electrons, subsequently the electrons bombard the phosphor screen where the electrons are converted into light again. Lastly the photons reaches the CCD screen, creating an image with wavelength on one axis and time on the other [19]. The streak camera possess two different modes: Focus and Operating mode. In focus mode the experimental settings are setup, such as amplification factor (how much the signal is amplified at the MCP), wavelength detection range as well as exposure time (the amount of time the CCD screen is open for exposure for the

converted photons), ultimately showing you an image of the emission with no time dependency. The Focus mode is essentially working as a fluorometer as it does not utilize the sweep electrodes, showing the emission spectra from the sample, whereas in operating mode the time dependency is measured with the sweep electrodes and the decay can be observed.

Optical Parametric Amplifier (OPA)

An OPA system's purpose is to allow the scientist to decide what excitation wavelength from a broad spectrum they desire to illuminate their sample. This section will go into detail how the OPA system, Harmony, used in this project works.

An instrument called the Jasper 10, generates a laser beam with a wavelength of $\sim$1030 nm which enters the OPA system. This beam interacts with a number of mirrors, crystals, beam splitters, filters and delay lines before it reaches the sample. The OPA system can be summarized in six parts, these parts are numbered in Figure 13 below. Before each part are illustrated there are some vital knowledge regarding super continuum generation, stimulated emission and harmonic generation needs clarifying.

As mentioned in the name, OPA, the desired wavelength is amplified, although first, the large range of wavelengths needs to be generated in order to choose which one is going to be amplified. This is where **Super Continuum Generation (SPCG)** plays a role. SPCG in simple terms means the conversion of monochromatic light into light with a broad bandwith, commonly referred as white light generation. SPCG can be achieved by sending femtosecond high intensity pulses of light into a material with nonlinear behaviour [21]. If the intensity of the pulse that's reaching the non-linear device is large enough, i.e, has a strong electric field, the Kerr effect takes place, which states that the materials refractive index change with a non-linear term that's intensity dependent [22] . The non-linear refractive index term gives rise to intensity and time dependent additional phase shift of the pulse called self phase modulation. Just how the Kerr effect give rise to a broadened spectrum is easiest explained with equations and correlating figures.

An ultrashort Gaussian laser pulse has the following intensity:

$$I(t) = I_0 * e^{(-\frac{t^2}{\tau^2})}, \tag{1}$$

where I_0 is the peak intensity and τ is equal to half pulse period.

A nonlinear material's refractive index, n, consists of two parts, the linear term, n_0 as

well as the nonlinear,$n_{nl}I$ which has a intensity dependence,

$$n(I) = n_0 + n_{nl} * I. \tag{2}$$

The nonlinear refractive index term causes a continuous phase change over the duration of the pulse

$$\begin{aligned} \phi(t) &= w_0 * t - k_0 * n(I) \text{ , where } k_0 = \frac{2\pi L}{\lambda_0} \\ &= w_0 * t - k_0 * (n_0 + n_{nl} * I(t)), \end{aligned} \tag{3}$$

where L is the propagation length, ω_0 and λ_0 is the frequency and wavelength of the pulse, respectively.

By calculating the time derivative of the phase, the intensity dependent frequency is illustrated

$$\begin{aligned} \omega(t) = \frac{d(\phi)}{dt} &= w_0 - k_0 * n_{nl} * \frac{dI(t)}{dt} \\ &= w_0 - k_0 * n_{nl} * \frac{-2t}{\tau^2} * I_0 * e^{(\frac{-t^2}{-\tau^2})} \\ &= w_0 + \frac{4\pi L n_{nl}}{\lambda_0 \tau^2} * t * I_0 * e^{(\frac{-t^2}{-\tau^2})}, \end{aligned} \tag{4}$$

along with an abbreviation of the nonlinear additional frequency change term,

$$w_{nl} = \frac{4\pi L n_{nl}}{\lambda_0 \tau^2} * t * I_0 * e^{(\frac{-t^2}{-\tau^2})}. \tag{5}$$

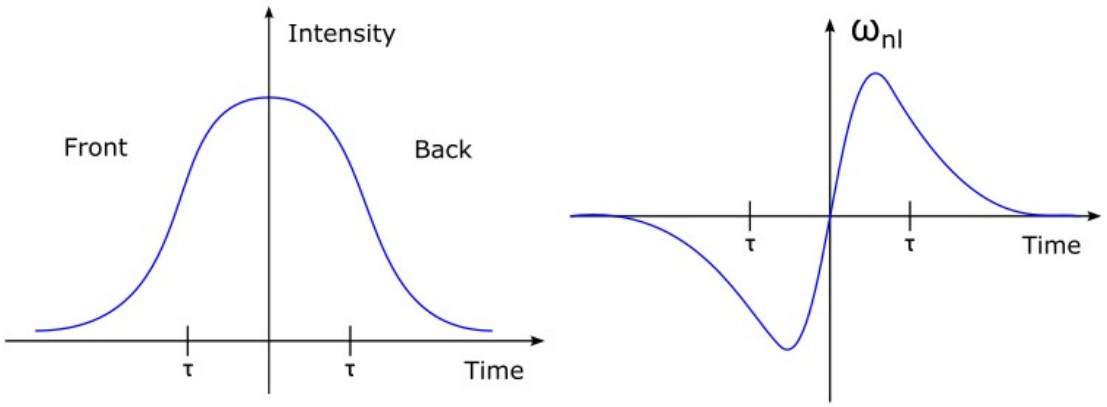

(a) **(b)**

Figure 10 a) A Gaussian laser pulse illustration and Figure b) Shows how the additional nonlinear frequency term changes over the course of the pulse.

Equation 4 along with Figure 10a shows that at the front of the pulse the time derivative of the pulse's intensity is positive and $t < 0$ this causes the additional nonlinear frequency, w_{nl}, to be negative which induces an continuous decrease of the frequency. Meanwhile when the opposite occurs, i.e. after the peak of the pulse, the intensity's time derivative is negative and $t > 0$, w_{nl} becomes positive and there is an continuous increase of the frequency. At time $t = 0$, w_{nl} is equal to zero meaning there is no frequency change at the peak of the pulse. Each position in time is demonstrated in Figure 10b above. As the intensity changes continuously during the pulse, this generates a broad spectrum with the pump's wavelength located in the center of the range. Since a nonlinear device with a fixed nonlinear refractive index n_{nl}, and thickness L, the equation 4 states that the frequency range depends on the pulse's wavelength, duration and intensity.

Photon amplification is commonly accomplished with the help of **Stimulated Emission (SE)**. When an excited electron relaxes and emits a photon with the energy corresponding to the materials bandgap, one refer this process as spontaneous emission. By exciting a material continuously, either with a laser pump or electrically, while another beam of light hits the crystal with a desired wavelength, the material may emit a so-called 'clone' photon in the same mode as the incoming light. This is called stimulated emission [23]. Resulting as shown in Figure 11, with two emitting photons that possess the same frequency, propagation direction, phase and polarization, ultimately amplifying the intensity.

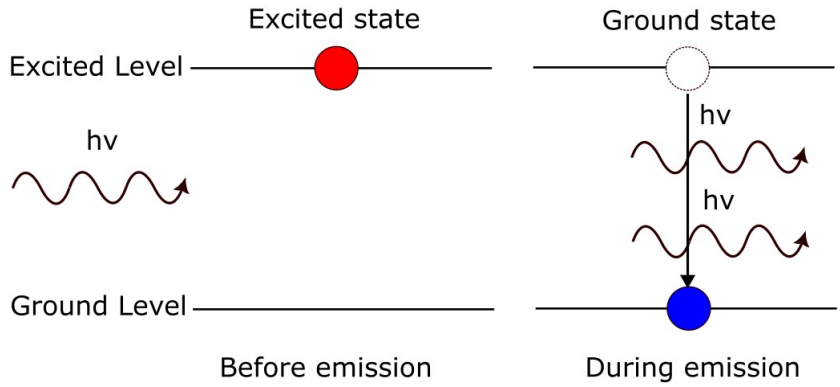

Figure 11 Illustration of Stimulated Emission.

In order to successfully generate a 'clone', the incident light, referred to as the 'Signal' always have a wavelength with lower energy than the pump that is used to excite the material. Since the incident wavelength is lower in energy than the bandgap there are some excess energy released, resulting with emission of a photon with a larger wavelength, this emission is referred to as the 'Idler'. The energy of the Signal and the Idler adds

up to the bandgap of the material, as shown in Figure 12, meaning altering the signal's wavelength will change the wavelength of the Idler.

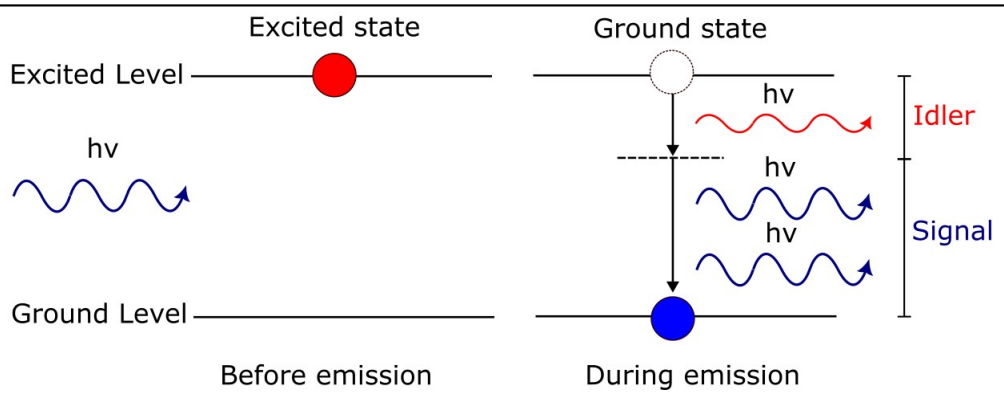

Figure 12 Demonstrates the generation of the Signal and Idler with the help of stimulated emission. The red ball represents a filled excited level due to excitation by the pump, whereas the blue ball represents a filled ground level. The dashed line corresponds to the energy level between the ground and excited level which equals the energy of the Signal. Where the excess of energy which corresponds to the difference between the dashed line and the excited level is the energy of the Idler.

With the help of stimulated emission, it is now possible to generate a wide range of wavelengths, using either the Signal or the Idler as the excitation wavelength. Although with an restriction an energy lower than the laser pump. In order to generate light with higher energy than the pump, **Harmonic Generation** is needed. Harmonic generation enables an increase of frequency, by utilizing a nonlinear device this can be achieved [24]. Doubling, tripling or quadrupling of the frequency are the most common, this OPA system offers an opportunity to generate the the second and fourth harmonic of both the Signal and the Idler. With the help of harmonic generation, this system that utilizes a laser with 1030 nm wavelength can generate wavelengths all the way down from 210 nm (fourth harmonic of the signal) up to 2600nm (Idler), all demonstrated in Figure 29 in the Appendix.

With that clarification of SPCG, SE and Harmonic generation, it is finally time to go through the schematics of the OPA system, visualized in Figure 13.

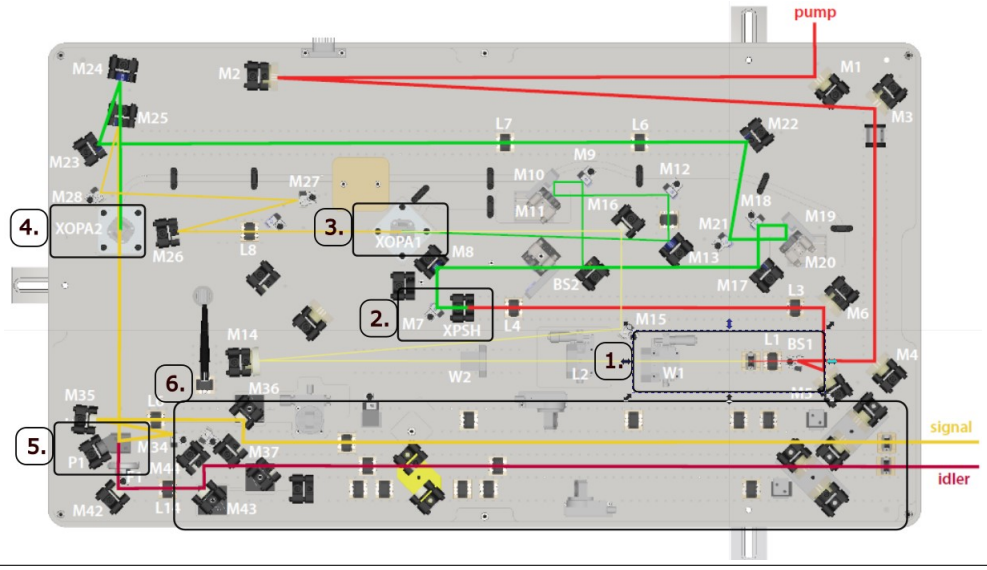

Figure 13 Schematics of the Harmony's OPA.

The laser beam enters the OPA in the top right corner and after some mirror reflections it arrives at checkpoint 1. Here, the beam splits up, where some of the light gets reflected and keeps its wavelength, this light is referred to as the pump for the amplification. The rest of the light hits W1 which is a nonlinear material causing a super continuum generation, i.e., white light generation. The pump continues to checkpoint 2 where with the help of another nonlinear device generates the second harmonic of the pump, $\sim$515 nm. The generated white light along with one part of the pump arrives at checkpoint 3 where stimulated emission occurs and the desired wavelength within the white light is amplified, creating a Signal and an Idler. This checkpoint is referred to as the first amplification, by changing the position and angle of the mirrors different wavelengths can be amplified. The amplified light along with the second part of the pump continues to checkpoint 4, referred to as the second amplification, which similarly utilizes stimulated emission. Both the Signal and Idler reaches checkpoint 5 where they get separated with the help of a beamsplitter. The last checkpoint 6 has mobile parts where you remove or add certain mirrors depending if harmonic generation is desired or not. Lastly both the Signal and the Idler exit the OPA system at the bottom right corner.

4 Method

4.1 Outline

The experimental part of the project consists of the following parts:

- Material synthesis and sample fabrication
- Optimizing the thickness of the intermediate layer between the plasmonic nanoparticles and the UPC material with the help of TRIR and UV-Vis measurements.
- Flourescensce measurements of solely the UPC to confirm fluorescence as well as having a baseline for the material.
- Evaluation of enhanced fluorescence with deposited plasmonic nanoparticles for the UPC material.
- Perform fluorescence measurements at different excitation wavelengths to gain a deeper understanding of available electronic states.
- Streak camera measurements to gather information about the excitation lifetime of the individual samples as well as observe if there is any upconversion.
- Complement with TCSPC measurements to gather additional information about the emission's lifetime.

4.2 Materials

The UPC samples consist of three thin film layers stacked upon each other. One layer of spray-deposited Au nanoparticles with size 8-12 nm as the plasmonic material, spincoated ZrO_2 as the intermediate layer with thicknesses varying approximately between 20-35 nm, and lastly spincoated ZnO with thickness of 20 nm as the UPC material.

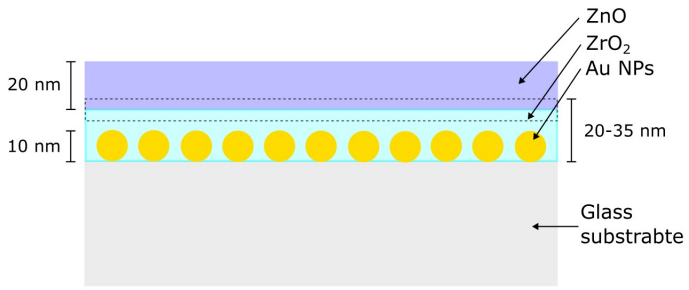

Figure 14 Illustration of the UPC samples and the respective thin film layers.

4.3 Material synthesis and sample fabrication

Chronological outline of the laboratory work creating the samples:

- Glass substrates were cleaned with the help of a sonicator and an ozone cleaner.
- The glass substrates were placed on a heater with a temperature of 350 °C, where deposition of gold on the surface using a spray gun were carried out. When sufficient amount of gold were deposited the samples were put in an oven with a temperature of 500 °C for one hour.
- Once more the samples were cleaned with the ozone cleaner and then spincoated with the different concentration ratio of the ZrO_2 and revolutions per minute. After spincoating the samples were put on a heater for 10 minutes at 150 °C and then again put in the oven but for 150 °C for 30 minutes.
- Same procedure as for the spincoating and heating of the ZrO_2 were carried out for the ZnO.
- The baseline samples without the gold nanoparticles were prepared in the same way except only spincoated with ZnO.

4.4 Choosing ZnO

Two different ZnO were used, defined as 'R' and 'S'. 'R' was a ZnO ink formulated for inkjet and slot die printing from GenesInk, commonly used as an electron transporting layer [25]. While 'S' was provided from Prof. Edvinsson's group at Ångström laboratory synthesised via wet chemical method [26]. In order to determine which one

that was more emissive than the other, samples with solely the different ZnO was prepared. These samples was then also used as a criterion to see if there was any enhanced fluorescence with the samples containing the plasmonic material.

4.5 Optimization of the intermediate layer

A total of six UPC samples were prepared with different modifications of the intermediate layer. Each sample's intermediate layer were spin coated with a modification regarding two parameters; concentration ratio and spin coated with different revolutions per minute, demonstrated in Table 1. The ceramic material ZrO_2, known for its wide bandgap and insulating properties, was diluted with water to create two distinct concentrations. The different concentrations consisted of one part ZrO_2 20 wt% which were then diluted with either five or ten parts water, resulting with either 3.3 wt% and 1.8 wt% respectively.

Table 1 The different concentration and rotations per minute for each sample.

Name	**Concentration** ZrO_2 [wt%]	**RPM**
P1	1.8	4000
P2	1.8	3000
P3	1.8	2000
P4	3.3	5000
P5	3.3	4000
P6	3.3	3000

4.5.1 Evaluation of the different parameters

To qualitatively observe if there were any charge transfer from the plasmonic material to the UPC material, TRIR measurements was made on each sample with different

intermediate layer parameter along with one sample with no intermediate layer, which were used as a baseline. Since the deposition of gold was sprayed manually by hand the gold concentration differ from sample to sample. To correlate the gold concentration for each sample to the amount of electrons excited in the TRIR measurements an UV-VIS spectroscopy measurement was carried out as well. The absorbance peak correlated to the gold nanoparticles for each sample were used as a normalisation factor. The gold concentration, i.e. the absorption peak of the sample with no intermediate layer was set to be the baseline and the other samples were normalized to this through observation their individual UV-Vis maximum absorption peak.

Fluorescence measurements with 300 nm as the excitation wavelength was carried out for the designated P1-P6 UPC samples. Together with the emission spectra and the normalized TRIR measurements the most favourable samples were chosen for another set of UPC samples. The chosen samples were P2, P5 and P6 and they were prepared similarly as mentioned before although with one alternation, two layers of spin coated ZnO instead of one, in order to achieve a greater thickness and increase the emission.

4.6 Mapping the available electron states and validating plasmon enhancement

4.6.1 Fluorescence measurements

Fluorescence measurements with the following excitation wavelengths were carried out for the second set of UPC samples; 300 nm, 400 nm, 500 nm, 550 nm and 600 nm. Firstly the samples were excited with 300 nm, this is above the band gap of the ZnO ($3.3eV, \approx 375nm$), hence the results should give an reflection of the materials emission [28]. Secondly the samples were excited with the other wavelengths ranging from 400 - 600 nm to evaluate if any of the intermediate states was available for excitation and to also achieve a better understanding of the emission. Identical fluorescence measurements was carried out for the samples containing solely the ZnO to verify any plasmonic enhancement of the emission.

4.7 Upconversion and lifetime observation

4.7.1 OPA and Streak camera setup

The Streak Camera at Uppsala University suffered some technological issues, resulting in problem shooting continuously throughout the project. Simultaneously a thorough

OPA calibration was carried out, meaning correlating the different positions and angles to each amplified wavelength and manually putting this into the software of the OPA system. The software could then automatically align the mirrors when any desired wavelength was set. Unfortunately the issues with the Streak Camera was never resolved and even though the OPA system was working it was never used for any measurements. Instead, a trip to Lund University was arranged and streak camera measurements were accomplished there.

4.7.2 Streak camera measurements

The Streak Camera setup at Lund University differed slightly, instead of using an OPA system that can generate a broad range of wavelengths the setup in Lund was restricted to an excitation wavelength of either 400 nm or 800 nm. In order to excite the hot carriers, consequently enhancing the electric field on the surface of the gold nanoparticles, another laser with an excitation wavelength in the gold's plasmon resonance frequency was needed. Therefore an extra Continous Wave (CW) laser with a wavelength of 532 nm was used aswell. Leading to streak camera measurements analyzing the difference of emission when illuminating the samples with solely the 400 nm laser as well as adding the 532 CW laser. The purpose of the Streak camera measurements was to observe any upconversion as well as investigate the longevity of the emission.

4.7.3 Time-correlated Single Photon Counting (TCSPC) measurements

Even though TCSPC measurements does not give information regarding the emission wavelength it was still just like the streak camera used to gather the lifetime of the emission. To qualitatively compare the fluorolog measurements with the TCSPC the same excitation wavelengths were used.

4.7.4 Fluorolog measurements

To complement the Streak Camera and the TCSPC measurements fluorescence measurements with excitation wavelengths 600 nm and 750 nm and detection range between 300 - 575 nm were carried out. The purpose of these measurements was to further evaluate if the ZnO has the available intermediate electron states needed for upconversion.

5 Results

5.1 Material synthesis and sample fabrication

Some difficulties were encountered during the creation of the samples. The spray gun changed it's deposition rate depending on the amount of liquid in the container as well as the spray not having an homogeneous trajectory which resulted in samples possessing a gold concentration gradient. This is shown in Figure 15 a), where the gold concentration appears to increase from right to left for both the P4 and P5 sample. Another difficulty when applying the gold nanoparticles was that if the spray deposition happened to quickly, the particles started to agglomerate and forming larger clusters of gold, which is shown in the second set of samples in Figure 15 b).

(a) **(b)**

Figure 15 a) Photo showing an gold concentration gradient, increasing from right to left. b) Image demonstrating larger clusters of gold due to rapid spray deposition.

The higher concentration of ZrO_2 appeared to be more viscous resulting in a less homogeneous film towards the edges of the sample as shown in Figure 16 a). Hence all the measurements were closely overlooked so that the incident light reached the center of the samples where the film thought to be more homogeneous. The deposition of ZnO had less issues and adequate films were accomplished for both the P1-P6 samples as well as the samples with solely ZnO which is displayed in Figure 16 b).

(a) **(b)**

Figure 16 a) Photo displaying how the higher viscosity of the ZrO_2 resulting in a less homogeneous film. b) A clear image of samples spin coated with only ZnO showing a satisfactory homogeneous film at the center.

5.2 The different ZnO's emissivity

Fluorescence measurements with excitation wavelength set to 300 nm (above the ZnO's bandgap $\approx 375nm$) were carried out for four samples, two of each ZnO (S and R). Figure 17 shows a significant difference in fluorescence between the different ZnOs, where the ZnO called S emits around ≈ 3 times greater than the one called R at the maxima. Therefore the second set of UPC samples was spin coated with the ZnO named S.

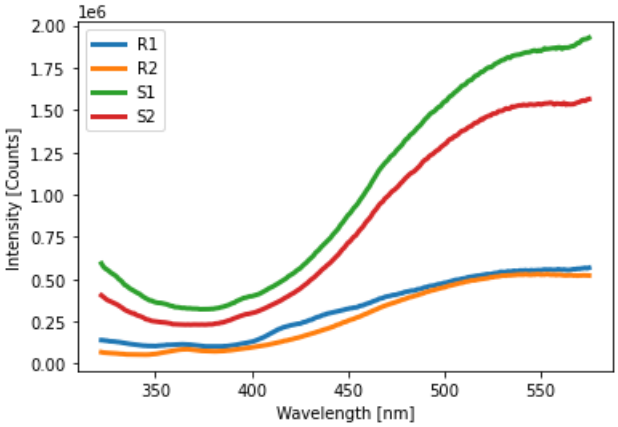

Figure 17 Fluorescence measurements with excitation wavelength of 300 nm for samples containing solely the two different ZnOs.

5.3 Opimization of the intermediate layer

5.3.1 UV-Vis absorbance measurements

Figure 18 shows the absorbance spectra for the P1-P6 samples along with one sample with No Intermediate Layer (NIL). The peak at $\approx$ 550 nm corresponds to the absorption of the gold nanoparticles, as it is their plasmon resonance frequency. The increase of absorbance around 375 nm corresponds to the band gap excitation of the ZnO while the absorption closer to 300 nm is most probably due to absorption of the glass substrate.

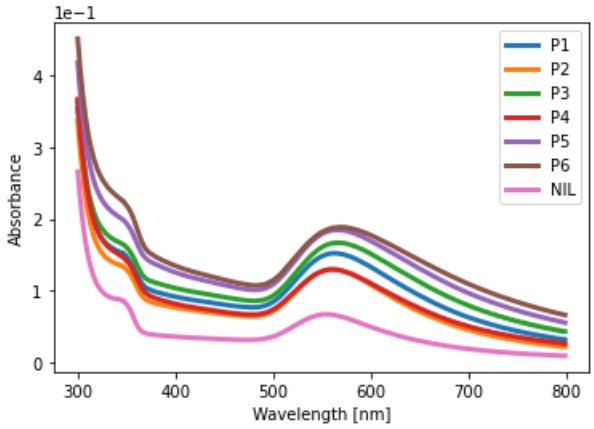

Figure 18 Absorbance spectra of P1-P6 samples as well as a sample without no intermediate layer (NIL).

5.3.2 TRIR spectroscopy measurements

Normalization factors for each P1-P6 sample were calculated from their absorption peaks and then related to the NIL sample's absorption peak, which was used as a baseline. In order to competently compare the TRIR measurements for each individual sample, the data points were normalized to their individual maximum value, resulting in each sample's peak is equal to one. Figure 19 shows TRIR measurements of each P1-P6 samples along with the baseline sample with no intermediate layer with normalization for both gold and intensity.

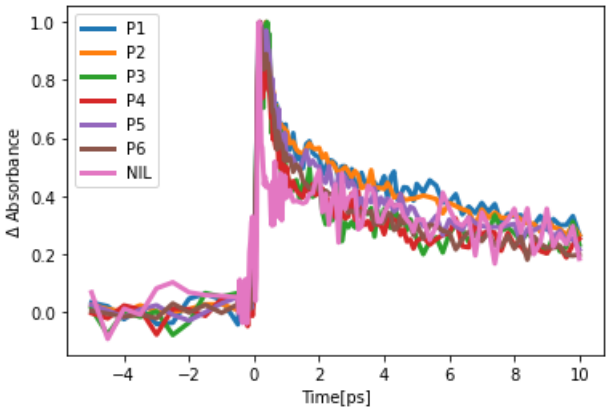

Figure 19 Graph showing the normalized time resolved absorbance of each P1-P6 sample along with a sample with no intermediate layer (NIL). The pump used for excitation had the wavelength of 550 nm, which is at the gold's plasmon resonance frequency, and the probe used a wavelength of 5000-5400 nm.

From the normalized TRIR spectra, Figure 19, it is shown that the absorption dropped off significantly quicker for the sample with no intermediate layer, indicating possible electron charge transfer between the gold and the ZnO. Another reason for the rapid decline could be a near field coupling with the ZnO which then quenches the plasmons faster. All the P1-P6 samples that contain an intermediate layer of ZrO_2 drops off more slowly, implying no electron charge transfer between the layers. As to why the noise for the NIL sample was noticeably larger may be a result due to a lower signal from the sample. Which also correlates with the lower concentration of gold for the NIL sample as demonstrated in the previous absorption spectra in Figure 18.

5.3.3 Fluorescence

Finally, in order to determine whether any of the P1-P6 samples' fluorescence was more or less enhanced by the gold nanoparticles, i.e. possessing the more appropriate intermediate layer parameters. Fluorescence measurements with 300 nm as the excitation wavelength for each sample were performed. Figure 20 shows the fluorescence spectra for each sample individually. The emission was broad and similar for all samples except P5 which stood out with a higher amount of fluorescence. To avoid the second harmonic peak the graph has a gap at 600 nm.

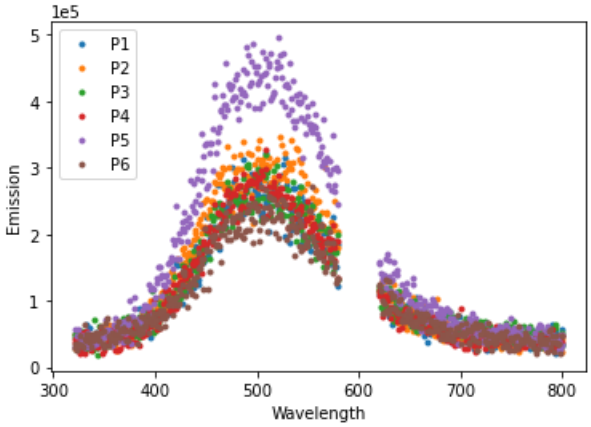

Figure 20 Fluorescence spectra with 300 nm as the excitation wavelength for each P1-P6 sample.

With the result from the UV-Vis, TRIR and Fluorescence measurements the samples P2, P5 and P6 were chosen for another set of samples with the same parameters, although with a double spin coated layer of the ZnO called S. P2 and P5 were chosen due to the ever so slight increase of fluorescence shown in Figure 20. Since the result is similar for all samples, P6 was chosen as well since it is supposed to posses the thickest and most dense intermediate layer (the 1:5 concentration and the lowest spin coating rpm). Meaning if the next set of P6 samples show similar results as P2 and P5 this could be an indicator that all the P1-P6 samples are in the thickness range which would prevent charge transfer as well as enhancement of the absorption and emission.

5.4 Plasmonic enhanced absorption and emission

Another UV-Vis absorbance spectra, Figure 21, was measured for the second set of P2, P5 and P6 samples along with a sample containing only spin coated ZnO (S) and a glass substrate (GSO, Glass Substrate Only) which all thin films were deposited on. A measurement of the GSO were performed to verify that none of the emission came from the substrate itself. The absorption is generally enhanced for all wavelengths and significantly at the gold nanoparticles plasmon resonance frequency.

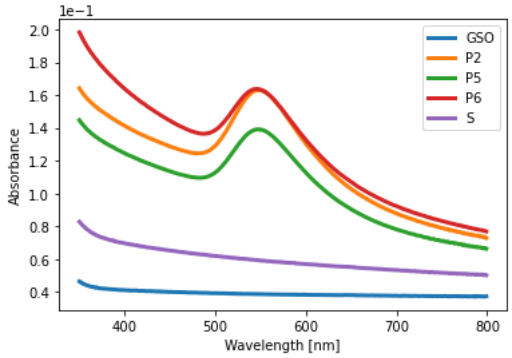

Figure 21 Absorbance spectra for the P2, P5, P6 , S and GSO samples.

Below five fluorescence emission graphs are presented, all for the same samples, P2, P5, P6, S and GSO. In Figure 22 a) and b) the excitation wavelength was 300 and 400 nm, respectively. While in Figure 23 a), b) and Figure 24 the excitation wavelength used were 500, 550 and 600 nm, respectively.

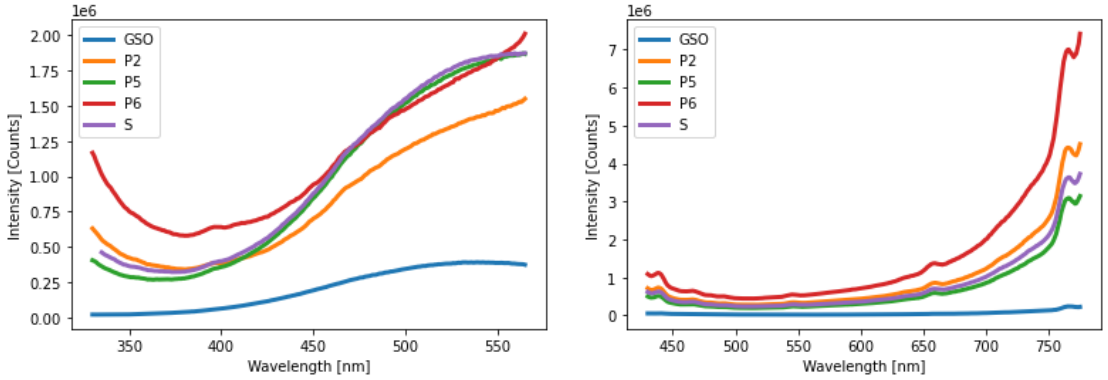

(a) **(b)**

Figure 22 a) Fluorescence spectra with excitation wavelength 300 nm. b) Fluorescence spectra with excitation wavelength 400 nm.

Figure 22 a) show a broad emission from both samples possessing plasmonic materials and not, which indicates no enhanced emission when exciting above the ZnO's bandgap. In the same graph it is evident that the glass substrate emits substantially less than samples with ZnO. Although the GSO also possess a broad emission around the same center as the samples with ZnO, which may be needed to have in mind when interpreting the data.

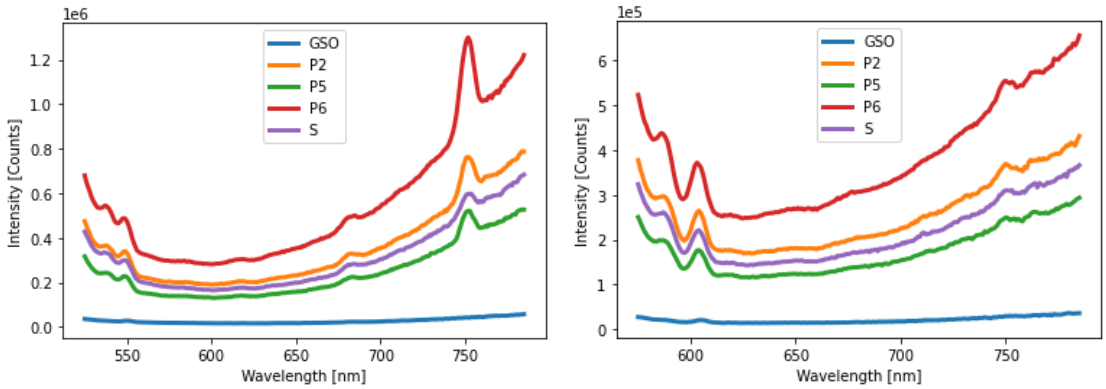

(a) **(b)**

Figure 23 a)Fluorescence spectra with excitation wavelength 500 nm. b) Fluorescence spectra with excitation wavelength 550 nm.

When exciting with energy less than the bandgap as shown in the rest of the graphs, ranging from Figure 22 b) to Figure 24 both P2 and P6 show enhanced emission compared to the S sample meanwhile P5 emits less. Ultimately showing an uncertainty regarding any plasmonic enhancement. Each of these graphs show an increase of fluorescence from 600 nm upwards to 800 nm, although significantly lower intensity, possibly indicating there is involvement with intermediate electron states when illuminating ZnO below it's bandgap energy. The various visible artifacts shown in all graphs through Figure 22 b) to Figure 24 are narrow, indicating that these peaks are probably related to the experimental setup and not available electron states.

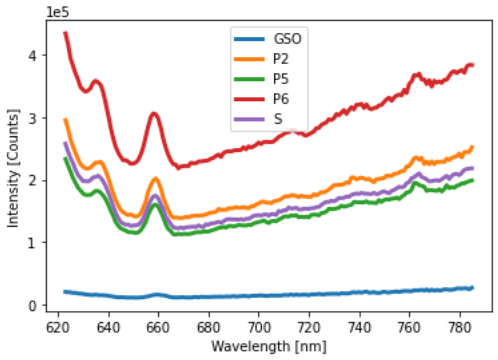

Figure 24 Fluorescence spectra with excitation wavelength 600 nm.

5.5 Emission lifetime and upconversion observation

5.5.1 Streak camera measurements

In the pursuit of observing potential upconversion with the streak camera at Lund University some problems occured. The lifetime of the emission from the sample was longer than the rate which the streak camera measures. Meaning no time resolved measurements in operate mode could be carried out. Instead measurements in focus mode which shows a fluorescence spectra were completed. To observe any enhancement from the plasmonic material, measurements were analysed with and without an additional 532 nm CW laser while exciting with 400 nm. Where the goal of the 532 nm CW laser was to excite the LSP's and enhance the electric field, as 532 nm corresponds to the region of the gold nanoparticles's plasmon resonance frequency, which should increase the absorption and emission of the ZnO. In Figure 25 a) below the green plot represents without the CW laser and the red plot with. As shown in Figure 25 b) which visualize the difference between the two plots, the intensity is low, meaning the plasmon enhancement is negligible when excited with 400 nm along with a 532 nm CW laser.

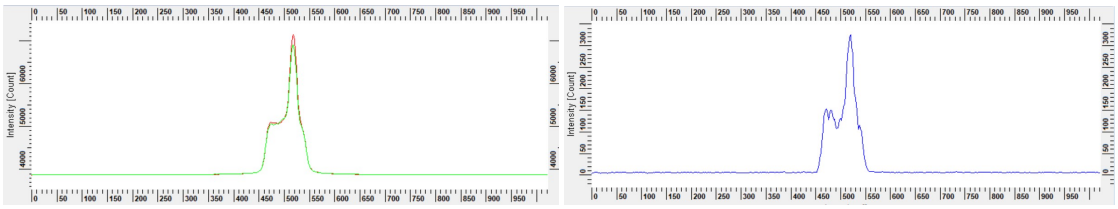

(a) **(b)**

Figure 25 a) Streak camera measurement in focus mode showing the fluorescence spectra with excitation wavelength 400 nm with(red) and without(green) 532 nm laser for the sample P6. b) Spectra visualising the difference between the two emissions, the green has been subtracted from the red.

Similar results were achieved with the P2 and P5 samples, shown in Figure 30 and 31 in attachments.

5.5.2 TCSPC measurements

The TCSPC analysis were unsuccessful due to experimental limitations regarding measuring solid films. The current experimental setup is not equipped with a holder compatible with solid films and lacking an integration sphere, which ultimately prevented any reliable time resolved measurement of low-emission samples as the ones in this project.

Conclusively the only information gathered surrounding the lifetime of the emission is the rate of the streak camera, which can only detect emission with lifetimes less than 12 ns, meaning that the lifetime must be longer than 12 ns.

5.5.3 Fluorescence measurements

In Figure 26 a) and b), corresponding fluorescence spectra with excitation wavelength 600 nm and 750 nm respectively is shown. No apparent evidence of any upconversion was presented, the sharp peak at $\approx$ 500 nm which is shown in both a) and b) most probably come from other sources than fluorescence, such as nonlinear effects and angle dependency.

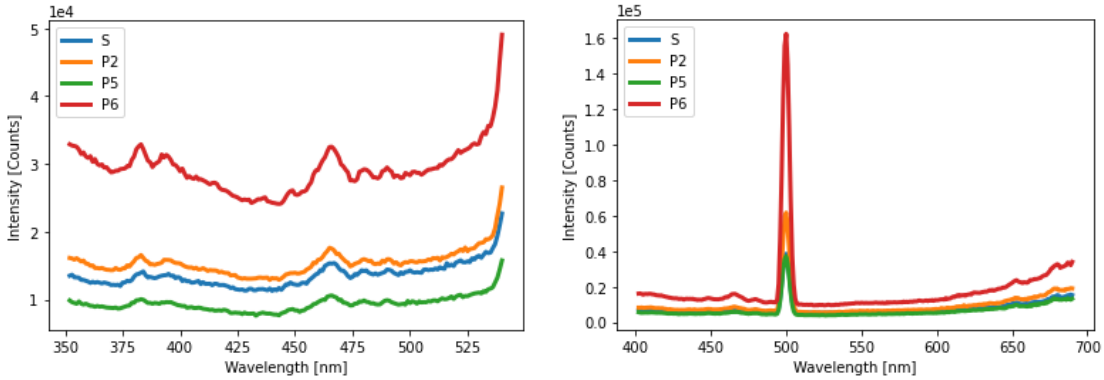

(a) **(b)**

Figure 26 a) Fluorescence spectra with excitation wavelength 600 nm. b) Fluorescence spectra with excitation wavelength 750 nm.

6 Discussion

6.1 The intermediate layer and plasmon enhancement

All the various intermediate layers did prevent charge transfer between the gold and the ZnO, interpreted from Figure 19, meaning that the film is thick and insulating enough. The increase of the emission for samples, P2 and P6 as shown from Figure 22 b) throughout to Figure 24, implies that the intermediate layer is thin enough for the ZnO to be effected by the plasmon enhanced electric field. Since there is evidence of none to low amount of charge transfer occuring between the layers the enhancement of the emission can it with high probability be established as a purely photonic process. Another important note is that the absorption also do seem to be enhanced over all wavelengths and not only at the gold's plasmon resonance frequency. As the enhancement due to plasmons are proportional to the absorption's amplitude, meaning that the enhanced absorption outside of the gold absorption peak may be related to other experimental setup or sample effects. Since the experimental setup only measures absorption as the lack of transmission through the sample, the reflection aspect is not taken into account. The increase of absorption outside of the gold's absorption peak may as well be explained by reflection caused by the large bandgap material ZrO_2, used as the intermediate layer.

One interesting case is the P5 sample which has a lower absorption shown in Figure 21, which can actually be due to a larger amount of reflection from the sample. As to why the P5 sample possibly has a larger reflection can be due to the spin coating inconsistency of the intermediate layer. Suggesting that the spin coating inconsistency of the ZrO_2 causes alterations in the amount of light absorbed by the gold. A different reason could be that the gold concentration is actually lower in the P5 sample, though the most probable reason may be a combination of the both. Sample P5 does not possess an enhancement of the emission either, in fact as shown from Figure 21 b) and throughout to Figure 23, it is actually lower than sample S, which consists of solely ZnO and no nearby plasmonic material. As to why P5 show less emission than a sample with solely ZnO need further investigations, where the synthesis procedure of the samples are the most probable factor regarding the unreliable result.

6.2 Upconversion

As shown from Figures 22 b) through Figure 24 it is apparent that intermediate electron states with an energy level below 600 nm are available for emission when exciting the

UPC samples with wavelengths possessing higher energy. Although electron states with a higher energy than 600 nm ($\approx$ 2.1 eV above the valence band) only seems to be available for emission when exciting above the bandgap, as shown in Figure 20 as well as Figure 22 a). That information could give one explanation as to why ZnO does not seem to have any upconverted emission when exciting with 600 nm and 750 nm as shown in Figure 26 a) and b).

In Figure 27 a) and b) an interpretation of the two cases are presented; a), exciting the UPC sample above the bandgap with 300 nm, b), exciting the UPC sample below the bandgap, with 600 nm. In the case of exciting above the bandgap as shown in Figure 27 a), the emission is broad, meaning there is nonradiative decay to the intermediate states inbetween the bands as indicated by thin horizontal lines, resulting in a wide emission range, where the highest intensity is located around 550 nm, as shown in the fluorescence measurements, Figure 22 a). From that result the hope was to with a low energy multiphoton absorption process achieve emission around that center. Instead when exciting with 600 nm and wavelengths with lower energy, nonradiative decay take place along with recombination and emission, interpreted from combining Figure 24 with Figure 26 a) and b). Ultimately in both Figure 26 a) and b), both Figures shows no sign of a second photon absorption i.e. upconversion when excited with a lower energy wavelength.

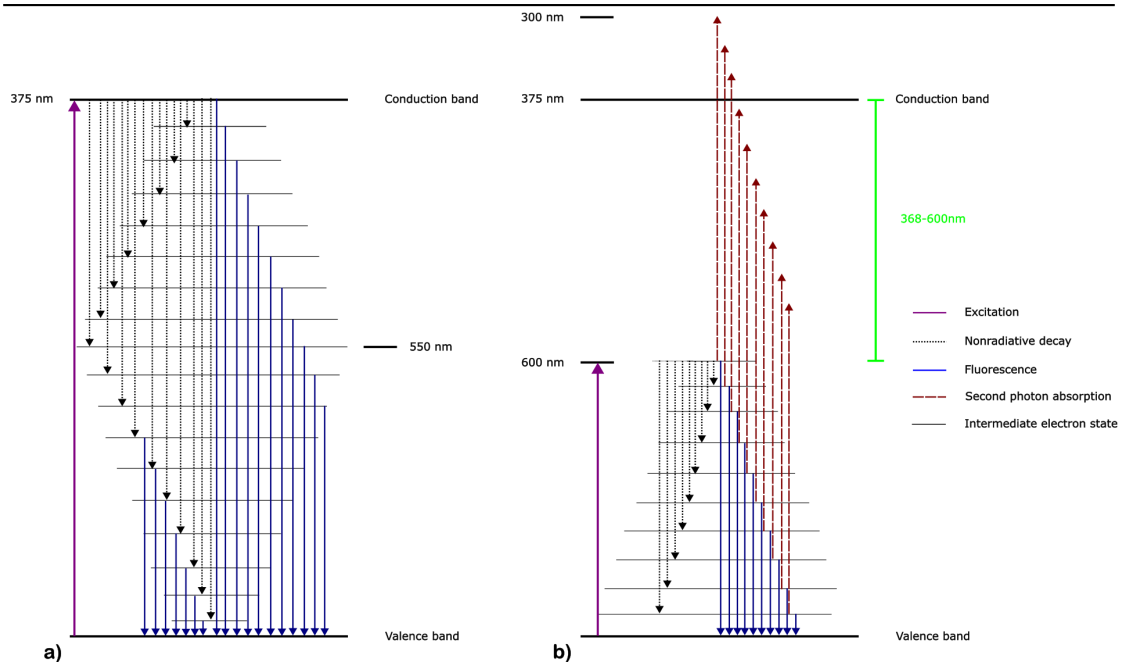

Figure 27 a) The nonradiative decay and fluorescence when exciting the UPC samples above the bandgap. b) The nonradiative decay and fluorescence when exciting the UPC samples with 600 nm, as well as a illustration of the multiphoton absorption process.

There could many reasons as to why upconversion does not happen. One is that the intermediate states above 600 nm are not available for photonic excitation and only available for nonradiative decay from excitations above the bandgap due to selections rule. Another reason is that the second photon absorption occurs with low probability and are not detectable above the noise level, where the low density of the intermediate states could play a role.

6.3 Future work

In future work regarding the pursuit of using ZnO for upconversion applications the most vital goal would be to enhance the density of available electron states for photon excitation. Which would increase the amount of absorption and therefore the fluorescence, which could result in a higher probability of a multiphoton absorption process, i.e. upconversion.

According to the following study "Significantly improved photoluminescnce properties of ZnO films by Lithium doping" one way to increase the photoluminescence is to dope the ZnO with Lithium [27].

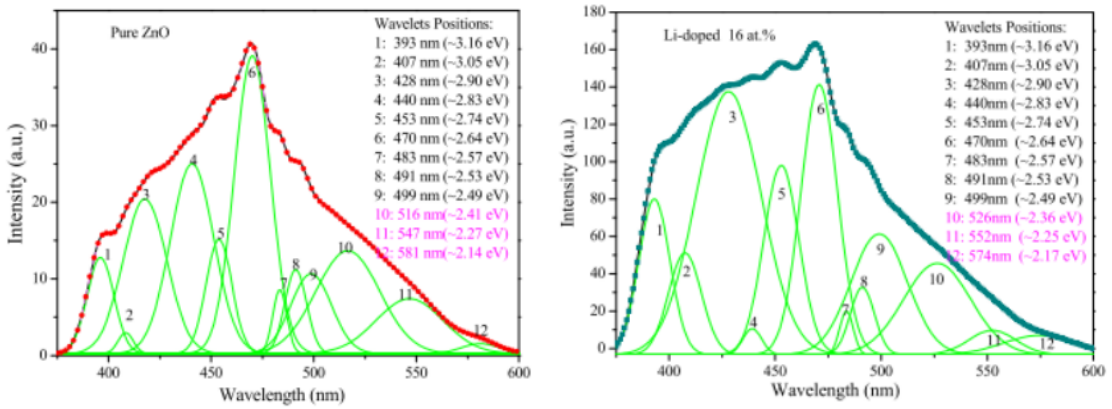

(a) **(b)**

Figure 28 a) Photoluminescence spectra showing the wavelet positions for pure ZnO. b) Photoluminescence spectra illustrating the enhanced fluorescence by Lithium doped ZnO [27].

Figure 28 a) shows the photoluminescence of their pure ZnO meanwhile Figure 28 b) shows the significantly enhanced photolumiscence of the ZnO when doped with 16 at.% Lithium. Taking this material and applying it to this project's research could make a large difference, as the density of the intermediate electron states are increased.

In future studies, the second focus should be to design the upconversion samples so that the plasmon enhancement of the field is pronounced. This could be done with more research regarding the spincoating and it's uncertainties as well as surface analysis.

With pronounced plasmon enhancement of the field, Lithium doped ZnO as well as a setup consisting of one laser with a wavelength in the gold's plasmon resonance frequency ($\approx 500 - 550nm$) and a laser with a wavelength in the IR region, optimal measurements can be done. The $\approx 500 - 550nm$ laser would then excite the gold, creating plasmons which would induce an increase of the surrounding electric field, supposedly leading to an even higher probability of an multiphoton absorption process of the IR light to occur.

7 Conclusions

- All the different intermediate layers of ZrO_2, separating the gold nanoparticles and the ZnO, with various spin coating parameters prevented any charge transfer from the gold nanoparticles to the ZnO.
- The gold nanoparticles´ enhanced surrounding electric field induced by plasmons showed an increase of photoluminescence for some of the samples and none for others. The uncertainty is most likely due to the synthesis processes, especially the intermediate layer consisting of ZrO_2.
- ZnO do possess intermediate electron states in between the valence and conduction band. The intermediate electron states with an energy level of $\approx$ 2.1 eV above the valence band (corresponding to 600 nm) is available for photon excitation, meanwhile the intermediate electron states above $\approx$ 2.1 eV and below the conduction band are not available for photon excitation unless exciting above the bandgap (3.3 eV), interpreted from the experimental fluorescence measurements.
- To determine whether ZnO is a suitable material for upconversion applications such as solar control windows further studies are needed. Additional research regarding how to optimise the functionality of the plasmonic material, gold, within the current thin film setup is required. By doping the ZnO with Lithium in order to increase it's photoluminescence, as well as using an experimental setup where exciting the gold with wavelengths that correspond to it's plasmon resonance frequency when simultaneously illuminating the samples with IR light would optimise the possibility of upconversion occuring.

8 Acknowledgements

I want to express my gratitude to a number of significant individuals that supported me throughout this project.

- My fellow colleagues in the office, who all always assisted me and created a great atmosphere.
  Thank you Robert Bericat Vadell, Vitor Silveira, Xianshao Zou and Ananta Dey.
- My knowledgeable and patient supervisor Jacinto for always helping me as well as challenging me. As well as my insightful subject reviewer Carl.
  Thank you Jacinto Sá and Carl Hägglund.
- I want to thank my girlfriend and friends who listened to me babbling on and on about my ups and down continuously throughout the project.
- Lastly I would like to thank my parents who has always supported me through every adventure of mine, I cannot begin to describe how thankful I am for you.

References

[1] SBBA Heating Market Report 2021
https://www.sbba.se/wp-content/uploads/sites/11/2021/09/Heating_Market_Sweden_2021_V1.0.pdf

[2] Monthly wholesale electricity prices in Sweden 2019-2023
Statista Research Department, 04-05-2023
https://www.statista.com/statistics/1271491/sweden-monthly-wholesale-electricity-price/

[3] Integration of smart windows into building design for reduction of yearly overall energy consumption and peak loads
Jean-Michel Dussault, Louis Gosselin, Tigran Galstian,
Solar Energy, Volume 86, Issue 11, 2012, Pages 3405-3416,
https://doi.org/10.1016/j.solener.2012.07.016.

[4] Down-conversion of UV radiation in erbium-doped gadolinium oxide nanoparticles
Anatoly Zatsepin, Yulia Kuznetsova
Applied Materials, Vol 12, Sep 2018, Pages 34-42
https://doi.org/10.1016/j.apmt.2018.04.001

[5] Enhancing the Photovoltaic Performance of Perovskite Solar Cells with a Down-Conversion Eu-Complex
L. Jiang, W. Chen†‡, J. Zheng, L. Zhu, L. Mo, et al.
ACS Appl. Mater. Interfaces 2017, 9, 32, 26958–26964
https://doi.org/10.1021/acsami.7b10101

[6] Ultrasfast Infrared-to-Visible Photon Upconversion on Plasmon/TiO2 Solid Films
Xianshao Zoua, Robert Bericat Vadell, Bin Cai, Xinjian Geng, Ananta Dey, Yawen Liu, Jie Meng, and Jacinto Sá

[7] Recent Advances of Plasmonic Nanoparticles and their Applications. Review
Jianxun Liu 1,2, Huilin He 1, Dong Xiao 1, Shengtao Yin 1,3, Wei Ji 3, Shouzhen Jiang 4, Dan Luo 1, J Materials Lett. 11(10), 1833 (2018)
https://doi.org/10.3390/ma11101833

[8] Plasmonic near-field absorbers for ultrathin solar cells
Hägglund, C. Apell, S. P. . J. Phys. Chem. Lett. 3, 1275-1285, (2012).
doi:10.1021/jz300290d

[9] Plasmon-Enhanced Upconversion
Di M. Wu, Aitzol García-Etxarri, Alberto Salleo, and Jennifer A. Dionne
The Journal of Physical Chemistry Letters 2014 5 (22), 4020-4031
https://doi.org/10.1021/jz5019042'

[10] Photon upconversion with hot carriers in plasmonic systems
Gururaj V. Naik and Jennifer A. Dionne , J Appl. Phys. Lett. 107, 133902 (2015)
https://doi.org/10.1063/1.4932127

[11] Plasmon-enhanced upconversion photoluminescence: Mechanism and application
J. Dong, W. Gao, Q. Han, Y. Wang, J. Qi, X. Yan, M. Sun
Reviews in Physics Vol 4 2019 https://doi.org/10.1016/j.revip.2018.100026

[12] Cushing, S. Plasmonic hot carriers skip out in femtoseconds. Nature Photon 11, 748–749
https://doi.org/10.1021/jz5019042

[13] Upconversion Plasmonic Lasing from an Organolead Trihalide Perovskite Nanocrystal with Low Threshold
Y-J. Lu, T-L. Shen, K-N. Peng, P-J. Cheng, S-W. Chang, M-Y. Lu, C-W. Chu, T-F. Guo, and H. Atwater ACS Photonics 2021 8 (1), 335-342
https://doi.org/10.1021/acsphotonics.0c01586

[14] Experimental Methods in the Physical Sciences
A. Christ , A. Fedrizzi , H. Hübel , T. Jennewein , C. Silberhorn Volume 45, Chapter 11-Parametric Down-Conversion, 2013, Pages 351-410
https://doi.org/10.1016/B978-0-12-387695-9.00011-1

[15] Recent Advances in Plasmonic Photocatalysis Based on TiO2 and Noble Metal Nanoparticles for Energy Conversion, Environmental Remediation, and Organic Synthesis
Ajay Kumar, Priyanka Choudhary, Ashish Kumar, Pedro H. C. Camargo, Venkata Krishnan
https://doi.org/10.1002/smll.202101638

[16] LibreTexts Chemistry
Physical Methods in Chemistry and Nano Science. Ch 4.4 UV-Visible Spectroscopy
https://chem.libretexts.org/Bookshelves/Analytical_Chemistry/Physical_Methods_in_Chemistry_and_Nano_Science_(Barron)/04%3A_Chemical_Speciation/4.04%3A_UV-Visible_Spectroscopy

[17] Principles of Fluorescence Spectroscopy
Joseph R.lakowicz, Ch.1 Introduction to Fluorescence, pages 1-4, 14-15 and 103-105.

[18] Mezzetti, A., Schnee, J., Lapini, A. et al. Time-resolved infrared absorption spectroscopy applied to photoinduced reactions: how and why. Photochem Photobiol Sci 21, 557–584 (2022).
https://doi.org/10.1007/s43630-022-00180-9

[19] Guide to Streak Cameras by Hamamatsu https://www.hamamatsu.com/content/dam/hamamatsu-photonics/sites/documents/99_SALES_LIBRARY/sys/SHSS0006E_STREAK.pdf

[20] Komura, M., Itoh, S. Fluorescence measurement by a streak camera in a single-photon-counting mode. Photosynth Res 101, 119–133 (2009).
https://doi.org/10.1007/s11120-009-9463-x

[21] Supercontinuum Generation, Nonlinear Optics, Dr. Rüdiger Paschotta https://www.rp-photonics.com/supercontinuum_generation.html

[22] Self Phase Modulation, Nonlinear Optics, Dr. Rüdiger Paschotta https://www.rp-photonics.com/self_phase_modulation.html

[23] Stimulated Emission, Nonlinear Optics, Dr. Rüdiger Paschotta https://www.rp-photonics.com/stimulated_emission.html

[24] High Harmonic Generation, Nonlinear Optics, Dr. Rüdiger Paschotta https://www.rp-photonics.com/high_harmonic_generation.html

[25] Company Genesink
https://www.genesink.com/heliosink/

[26] Energy Alignment of Quantum-Confined ZnO Particles with Copper
J. Thyr, J. Montero, L. Österlund and T. Edvinsson ACS Nanoscience Au 2022 2 (2), 128-139
https://doi.org/10.1021/acsnanoscienceau.1c00040

[27] Significantly improved photolumincescence properties of ZnO films by lithium doping
Xiangliu Chenb ,Xie Qingshuanga, Li Jitaoc
Jour. Ceramics International, Vol. 46, pg. 2309-2316 (2020)
https://doi.org/10.1016/j.ceramint.2019.09.220

[28] Band gap engineered zinc oxide nanostructures via a sol–gel synthesis of solvent driven shape-controlled crystal growth
K. Davis, R. Yarbrough, M. Froeschle, J. Whitea and H. Rathnayake.
Jour. RSC Advances, Issue 26, 2019
https://doi.org/10.1039/c9ra02091h

Appendix

Parameter	Value	Unit
Required input pumping beam		
wavelength	1030 ± 5	nm
pulse duration	< 300	fs
pulse energy at 200 kHz	35	µJ
beam size *w*, collimated	2	mm
polarization	linear, vertical	
beam quality M^2	< 1.5	
Output beams		
pulse duration	< 300	fs
beam quality M^2	< 1.5	
signal		
wavelength	630 – 1020	nm
min. pulse energy	> 0.8	µJ
pulse energy at peak of tunning range	> 2	µJ
polarization	linear, vertical	
idler		
wavelength	1040 – 2600	nm
min. pulse energy	> 0.3	µJ
pulse energy at peak of tunning range	> 0.8	µJ
polarization	linear, horizontal	
second harmonic of the signal		
wavelength	315 – 510	nm
pulse energy at peak of tunning range	> 0.7	µJ
polarization	linear, horizontal	
second harmonic of the idler		
wavelength	520 – 630	nm
polarization	linear, vertical	
fourth harmonic of the signal		
wavelength	210 – 250	nm
pulse energy at peak of tunning range	> 0.175	µJ
polarization	linear, vertical	
fourth harmonic of the idler		
wavelength	260 – 310	nm
polarization	linear, vertical	
fixed fourth harmonic of the pump		
wavelength	257 ± 2	nm
pulse energy	> 1.75	µJ
polarization	linear, vertical	

Figure 29 Image showing which wavelengths the OPA system can be generate with either the Signal or the Idler.

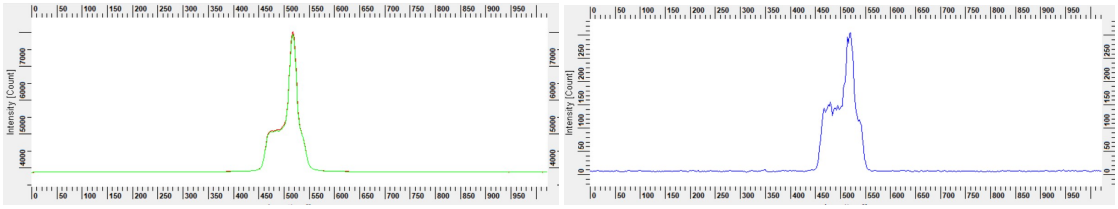

(a) **(b)**

Figure 30 a)Streak camera measurement in focus mode showing the fluorescence spectra with excitation wavelength 400 nm with(red) and without(green) 532 CW laser for the sample P2. b) Spectra visualising the difference between the two emissions, the green has been subtracted from the red.

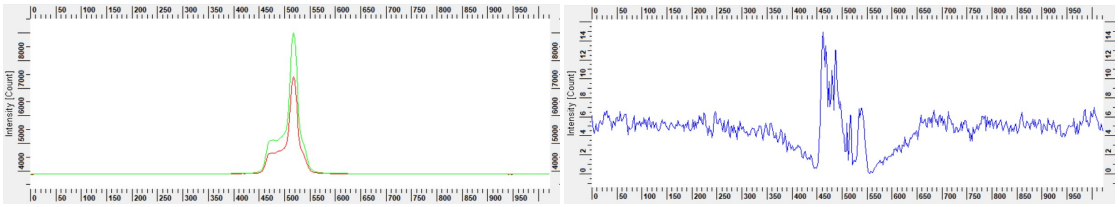

(a) **(b)**

Figure 31 a)Streak camera measurement in focus mode showing the fluorescence spectra with excitation wavelength 400 nm with(red) and without(green) 532 CW laser for the sample P5. b) Spectra visualising the difference between the two emissions, the green has been subtracted from the red.